Photo-inactivation of bacteria in hospital effluent via thiolated iron-doped nanoceria

Sara Khan[1], Sulaiman Faisal[1], Dilawar Farhan Shams[2], Maryam Zia[1], Akhtar Nadhman[1] ✉

[1]*Institute of Integrative Biosciences CECOS University, Peshawar, Pakistan*
[2]*Department of Environmental Sciences, Abdul Wali Khan University, Mardan, Pakistan*
✉ *E-mail: nadhman@cecos.edu.pk*

Abstract: Hospital wastewater is a major contributor of disease-causing microbes and the emergence of antibiotic resistant bacteria. In this study, thiolated iron-doped nanoceria was synthesised and tested for killing of microbes from hospital effluent. These particles were designed to inhibit the efflux pumps of the bacteria found in hospital effluent with further ability to activate in visible light via iron doping thus generating tunable amount of reactive oxygen species (ROS). The quantum yield of the ROS generated by the nanoceria was 0.67 while the ROS types produced were singlet oxygen (36%), hydroxyl radical (31%) and hydroxyl ions (32%), respectively. The particles were initially synthesised through green route using *Foeniculum vulgare* seeds extract and were annealed at 200°C and further coated with thiolated chitosan to enhance the solubility and efflux pump inhibition. X-ray diffraction confirmed the polycrystalline nature of nanoparticles and uniform spherical shape with 30 nm size, confirmed by scanning electron microscope. The nanoparticles exhibited 100% bactericidal activity at 100 μg/mL against all the isolated bacteria. The enhanced bactericidal effect of iron-doped nanoceria could be attributed to efflux inhibition via thiolated chitosan as well as the production of ROS upon illumination in visible light, causing oxidative stress against microbes found in hospital effluent.

1 Introduction

Hospitals generate large volumes of liquid effluent from heavy consumption of water usually 400–1200 L/d per bed [1]. Hospital effluent contains various pollutants such as drug residues, biological liquids, disinfectants, detergents, radiant elements, metals, X-ray contrast agents, a wide array of chemicals and pathogenic microbes that poses a serious environmental concern with potential effluent toxicity of 5–10 times higher than municipal wastewater [2, 3]. Of more concern in the effluent is the presence of disease causing bacteria particularly those resistant to antibiotics due to unnecessary or over use of antibiotics [4–6]. Hospital effluent is considered as the most significant source of disease-causing microorganisms such as *Salmonella*, *Shigella* and *Escherichia coli*, influenza virus, norovirus, Candida species, multidrug resistant *Staphylococcus aureus* and vancomycin resistant enterococcus [7–9]. The presence of these bacteria is linked to various diseases while the emergence of antibiotic resistant bacteria (ARB) has been considered among the principal public health concerns of the 21st century [10]. A major public health issue is the spread of infections especially diarrhoea, giardiasis, dermatitis, urticarial and many others [11]. Removal of these pathogenic bacteria and ARB is therefore imperative to avoid the related ecological and human health consequences.

Hospital effluent is generally discharged directly into urban sewage systems without prior treatment where they are conveyed and treated in conventional sewage treatment plants (STPs). Common treatment methods adopted in STPs include preliminary treatment, primary or physical treatment such as clarification and biological treatment such as activated sludge process, extended aeration, fluidised bed reactor, submerged aeration fixed film reactor, membrane bioreactor, sequential batch reactor and biological nutrient removal processes. These often are proceeded by a polishing step, e.g. disinfection [3, 12]. These methods are good at removing organic matter, nutrients (such as nitrogen and phosphorus) and suspended matter but not effective enough to remove constituents from hospital effluent such as pharmaceuticals, other trace organics, X-ray media and microbial load that not only show strong resistance to treatment but can also potentially inhibit biological treatment by 7–8% [2, 13]. Further, these STPs have been identified as the major source of antibiotics release and ARB [14, 15]. On the other hand, point source treatment processes for eradication of microorganisms from hospital effluent such as chlorination, UV irradiation, Fenton oxidation, ozonation and photolysis are cost-prohibitive for large-scale application [16, 17]. Moreover, in developing countries such as Pakistan, hospital effluent is directly discharged in sewage to surface water bodies without any treatment.

Hence, there is a great need to develop ecofriendly, cost-effective and efficient methods for the treatment of hospital effluent specifically targeting the removal of microbes. In this regard, nanotechnology can be considered as a significant area because of unique physiochemical characteristics. Recently, metal nanoparticles have been used as excellent biocidal agents for microbes [18]. Among them, cerium oxide, a rare earth oxide material [19, 20] is a semiconductor having 3.19 eV large energy bandgap with broad excitation energy of exciton [21]. Cerium oxide nanoparticles or nanoceria in bulk can be in two distinct forms; Ce^{4+} or Ce^{3+} as CeO_2 and/or Ce_2O_3, respectively, while in nanoform the structure of nanoceria is cubic fluorite on the surface of which both Ce^{4+} and Ce^{3+} synchronises. Due to the presence of Ce^{3+}, deficiency of charge is indemnified by intrinsic oxygen defects that play an important role in the catalytic process [22]. Addition of dopant (metal and/or transition metal) to the metal oxide nanoparticles produces surface defects, therefore enhancing the photocatalytic properties of nanoparticles. Surface defects and surface area in nanomaterials have significant impact on the efficiency of photocatalytic activity. The more the defect sites more electrons will be trapped, resulting in increase in the efficiency of photocatalysis [23], which further leads to generation of reactive oxygen species (ROS), which is considered as one of the most important way of causing cytotoxicity.

In this study, nanoceria have been synthesised using *Foeniculum vulgare* seeds extract and antimicrobial activity of thiolated chitosan (TC) iron-doped nanoceria was evaluated against microbes found in hospital effluent.
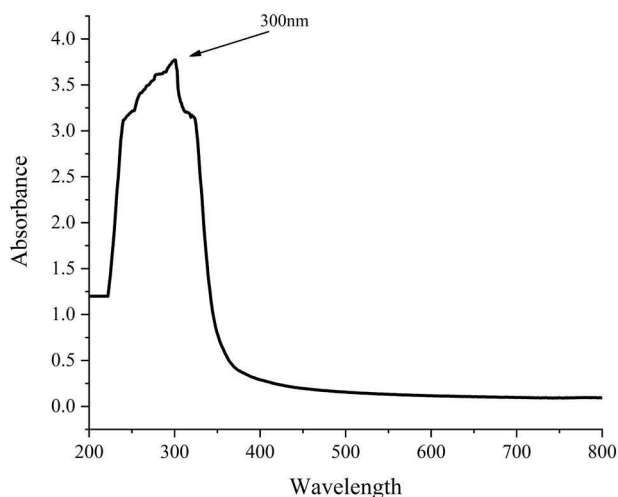
Fig. 1 *UV–visible absorption spectrum of iron-doped nanoceria*

2 Materials and methods

2.1 Chemicals and reagents

Cerium (III) nitrate hexahydrate $(Ce(NO_3)_3.6H_2O)$, iron (III) chloride hexahydrate $(FeCl_3.6H_2O)$ Triton X-100, sodium azide (NaN_3) and mannitol were purchased from Scharlau, Spain. 1,3-Diphenyl-isobenzofuran (DPBF), TC [24], ethanol, acetic acid and dimethyl sulphoxide (DMSO) were purchased from Analar. Phosphate-buffered saline, Luria broth and nutrient agar from Oxoid, UK.

2.2 Synthesis of iron-doped nanoceria

For nanoceria synthesis, *F. vulgare* (fennel) seeds were brought from local market and washed with distilled water several times to remove the dust. Later, 10 g of fennel seeds were suspended in 100 mL of distilled water and boiled for 10 min at 80°C. Afterwards, the mixture was filtered with Whatman No. 1 filter paper (0.45 μm) and stored at room temperature for further usage.

For the synthesis of 10% iron-doped cerium oxide nanoparticles, cerium nitrate (45 mM) and ferric chloride (5 mM) solutions were mixed and then 100 mL of plant extract was added and the solution was placed on magnetic hotplate at 300 rpm for 2 h at 30°C. After that, the solution was centrifuged at 9000 rpm for 15 min at 37°C followed by two times washing with distilled water and one time with 70% ethanol for 5 min each. The nanoparticles obtained were dried in an oven at 90°C for 2 days and then annealed at 200°C for 3 h [25].

2.3 Coating of iron-doped nanoceria

TC was used as a coating material for iron-doped cerium oxide nanoparticles. For coating, 0.1% of TC was dissolved in 1% acetic acid while equal quantity of nanoceria was sonicated in de-ionised water for 1 h. The TC was mixed with the dispersed nanoparticles solution and placed on a magnetic hotplate, stirred at 200 rpm and 30°C for 16 h. The solution was then centrifuged at 9000 rpm for 15 min and afterwards, washed twice with de-ionised water.

2.4 Characterisation of nanoceria

The crystalline structure of nanoceria was analysed by powder X-ray diffraction (XRD) (JDX-3532 JEOL, Japan) using CuKα radiation of wavelength 1.5418, current 30 mA and voltage 40 kV. For size and shape determination, scanning electron microscopy (SEM, JSM5910, JEOL, Japan) was performed. UV–visible spectroscopy (Thermo scientific Multiscan Go) in the range 200–800 nm was performed to analyse the respective surface plasmon resonance (SPR) of nanoceria. FTIR on TENSOR 27™ Bruker (Milan, Italy) was used to analyse the role of plant metabolites in the synthesis of nanoceria.

2.5 ROS quantification of TC-coated iron-doped nanoceria

For quantification of ROS, 0.2 mM solution of DPBF was prepared in ethanol. The dispersed nanoparticles (1 mg/mL) were added to 1 mL of DPBF solution in cuvette securely covered with parafilm, and exposed to LED light (84 lm/W) for 30 s. After each exposure, absorbance at 410 nm was measured by spectrophotometer (Thermo scientific Multiscan Go). Photobleching of DPBF occurred when exposed to light which resulted in decline of absorbance value at 410 nm. Methylene blue was used as a standard [26].

2.6 ROS moieties detection

It is considered that nanoceria might be generating singlet oxygen and hydroxyl radical [27]. To confirm that, 1 mM sodium azide, 1 mM mannitol [28] and 5% DMSO were used for singlet oxygen, hydroxyl radicals and hydroxyl ions, respectively. Four sets of reactions were carried out. Initially, nanoparticles and DPBF along with 1 mM sodium azide for singlet oxygen, while in the second set; nanoparticles dye and 5% DMSO for hydroxyl ion, in third set; 1 mM mannitol for hydroxyl radical detection. While in the fourth set (control), sodium azide, mannitol and DMSO were added in the DPBF dye solution along with the nanoparticles. Each of the respective set was exposed to LED light (84 lm/W) for 5 min and absorbance was measured at 410 nm.

2.7 Photo-inactivation of microbes

For the experiment, real hospital effluent was collected from Hayatabad Medical Complex, Peshawar, Pakistan. For viable count assay, 100 μL of 10 times diluted effluent sample was taken in a micro-centrifuge tube and nanoparticles were added in different concentrations of 100, 50 and 25 μg/mL. The tubes were incubated in shaking incubators for 60 min, then exposed to LED light while other in dark for 15 min and again incubated for 1 h while shaking at 37°C. Afterwards, 100 μL of each concentration was spread on nutrient agar plates using sterilised spreader and 100 μL diluted effluent sample (10 times) without nanoparticles was used as a positive control. The plates were incubated for 24 h at 37°C. Colony forming units were calculated from the ratio of number of colonies and amount plated (mL) multiplied by the dilution factor.

2.8 Efflux pump (EP) inhibition

Cartwheel assay was performed for real hospital effluent bacteria to determine the efflux inhibitory effect of TC-coated iron nanoceria. In cartwheel assay, bacteria expel ethidium bromide (EtBr) which is a common substrate for many EPs (transporter proteins). Within the cells, EPs inhibitors lead to accumulation of EtBr and produce fluorescence. Bacteria, EtBr and nanoparticles were taken in concentration of 50 μL each in a microcentrifuge tube. A dipped swab of this mixture was swabbed on the surface of nutrient agar plates in a cart wheel pattern. For control, bacteria and EtBr were swabbed on nutrient agar plates in cartwheel pattern. The plates were incubated overnight at 37°C. After incubation the plates were observed for fluorescence under UV transilluminaor [29, 30].

2.9 Data analysis

All the experiments were performed at least three times to ensure their reproducibility. The data from all these experiments were presented as mean with standard deviation. For data analysis and graphs, OriginPro 2018 (Origin-Lab) software was used.

3 Results and discussion

3.1 Characterisation of nanoceria

UV–visible spectroscopy of iron-doped nanoceria was performed in the range 200–800 nm. The absorbance peak was observed at 300 nm (Fig. 1), which is the respective SPR peak of nanoceria. For determination of functional groups involved in reduction and capping of nanoceria, Fourier transform infrared (FTIR)
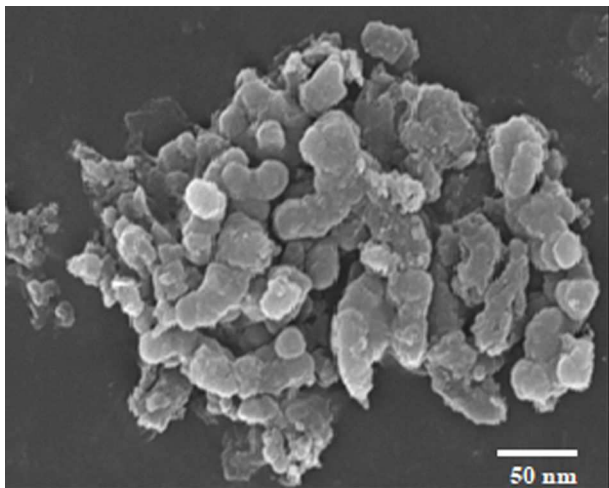
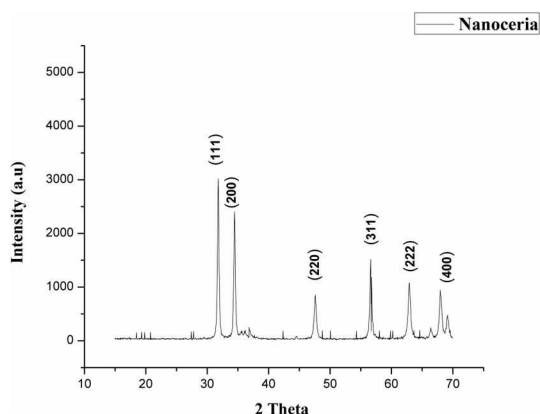**Fig. 2** *SEM image of nanoceria with average size of 30 nm*

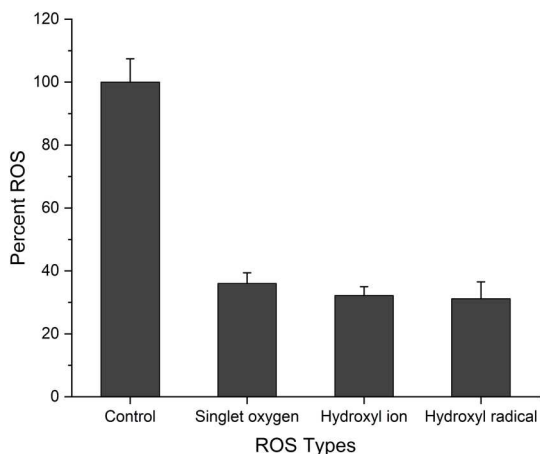**Fig. 3** *XRD pattern of polycrystalline iron-doped nanoceria*

Fig. 4 *Per cent production of ROS moieties by iron-doped nanoceria using 1 mM sodium azide for singlet oxygen, 5% DMSO for hydroxyl radical and 1 mM mannitol for hydroxyl ion*

spectroscopy was performed and compared to FTIR spectrum of fennel seeds adopted from Choudhary *et al.* [31], where absorbance band at 3345.66 cm^{-1} belongs to hydrogen bonded phenolic groups, 2928.30 and 2852.83 cm^{-1} belongs to asymmetric and symmetric stretching of methyl group and 1711.02 cm^{-1} corresponds to carbonyl (C=O)group. The FTIR spectra of nanoceria showed peaks at 3283.63 cm^{-1} which corresponds to OH, the two groups (at 2928.30 and 2852.83 cm^{-1}) completely disappeared and a new group formed at 1634.77 cm^{-1} corresponds to nitro group instead of 1711.02 cm^{-1} (C=O). This comparison suggests involvement of some phytoproteins, which are present in fennel seeds, in synthesis of cerium oxide nanoparticles.

The synthesised nanoceria were ellipsoidal in shape and were 30 nm in size (Fig. 2). XRD graph showed relatively close peaks to the CeO$_2$ fluorite structure (Fig. 3). The sharp intensity peaks at 2θ = 31.83, 34.42, 47.5, 56.75, 62.93 and 69.11 corresponded to (111), (200), (220), (311), (222) and (400) planes, respectively, which approves the polycrystalline nature of nanoceria. There are also a few impurity peaks in the XRD, which may be corresponding to the presence of plant metabolites on the surface of nanoceria.

3.2 ROS quantification and identification

The number of ROS produced was quantified using DBPF fluorescent dye as a chemical quencher and methylene blue was taken as standard. The quantum yield of nanoceria was calculated using the following formula:

$$\Phi\Delta CeO_2 = \Phi_{MB}(k_{CeO_2}/k_{standard}),$$

where $\Phi_{\Delta CeO2}$ and Φ_{MB} are the quantum yields of iron-doped nanoceria and methylene blue, respectively. The quantum yield of iron-doped nanoceria (k_{CeO2}) was quantified as 0.67 which was higher than standard quantum yield of 0.52 for methylene blue.

In type II photodynamic reaction, initially singlet oxygen is formed, which gives rise to other ROS moieties such as hydroxyl radical (OH·) [32]. Generation of these ROS moieties occurs when nanoparticles are illuminated with light having energy equal to or higher than the band gap, the electrons jumps from the valance band to the conduction band leaving a hole in the valance band. The holes in valance band exhibit high oxidative capability while electrons in the conduction band exhibit reducing power resulting in ROS production [33]. These ROS moieties result in oxidative stress leading to cell death. To determine the per cent contribution of various ROS moieties, different quenchers were used such as 1 mM sodium azide (NaN$_3$) for singlet oxygen ($^1O_2$), 5% DMSO for hydroxyl ion (OH$^-$) and 1 mM mannitol for hydroxyl radical (OH$^\cdot$). The type of ROS produced by iron-doped nanoceria in higher quantity was singlet oxygen (36%), followed by hydroxyl ion (32.2%) and hydroxyl radical (31.2%). Sodium azide, DMSO and mannitol in combination were used as a control (Fig. 4).

3.3 Photo-inactivation of microbes in hospital effluent

Plate count method was used for evaluation of antimicrobial activity of iron-doped nanoceria against microbes found in hospital effluent. Iron-doped nanoceria were added in concentrations (25, 50 and 100 μg/mL), while treatment without nanoparticles was taken as a control. Numbers of colonies found at concentration 25, 50 μg/mL were less compared to the control (dark and in water) while at higher concentration of 100 μg/mL, no colonies were detected. As shown in Fig. 5, continuous reduction in the number of colonies was observed with the increasing nanoparticles concentration. Primarily, the nanoceria bactericidal activity can be attributed to electrostatic attraction between negatively charged cell surface of bacteria and positively charged nanoparticles. However, ROS generation plays an important role in bactericidal activity. Various ROS species contributes in oxidative stress such as singlet oxygen ($^1O_2$), hydroxyl radical and super oxide anion radical which is less toxic compared to the other two species in biological systems [33, 34]. It is also believed that interaction of ions released from nanoparticles with surface proteins (S-H) group results in surface protein denaturation causing loss of protein permeability, eventually leading to cell death [34]. In the current study, the possible mechanism for antimicrobial activity could be synergistic effect of both thiolation and ROS as the thiolated iron-doped nanoceria generated higher number of ROS (0.67) especially singlet oxygen $^1O_2$, hydroxyl radicals and hydroxyl ions. Thiolation increased the retention of nanoceria in the bacteria cell thus by blocking the EP while, the ROS moieties resulted in oxidative stress leading to cell death.
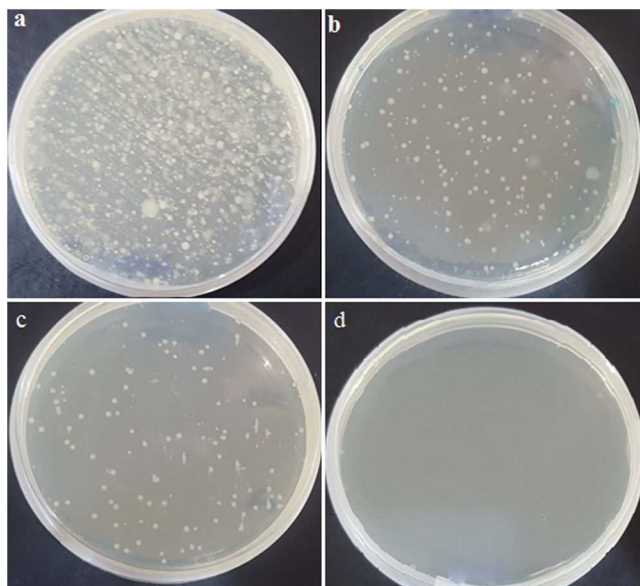
Fig. 5 *Plate count assay for antimicrobial activity of nanoceria against hospital effluent*
(a) Control with no nanoparticles, *(b)*, *(c)* Colonies observed at 25 and 50 μg/mL, *(d)* Complete eradication at 100 μg/mL
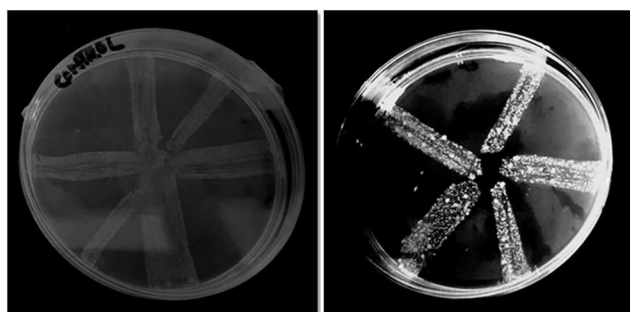

Fig. 6 *EP inhibition by iron-doped nanoceria in bacteria*

3.4 EP inhibition

In order to determine whether iron-doped nanoceria can inhibit EP, cart wheel assay was performed bacteria of hospital effluent. EPs are transporter proteins that expel the antimicrobial agents making bacteria resistant. As EPs transport noxious agents against the concentration gradient, they require energy sources to perform its functions. Most of the distinct EP families utilise the two instant sources of energy that is adenosine triphosphate and proton motive force (PMF) [35]. Previous studies have suggested that metal nanoparticles affect PMF. According to Christena *et al.* [29], metal nanoparticles possibly interfere with respiration of bacteria dissipating PMF. In this method, EtBr was used which serve as a substrate for bacterial EPs. Fig. 6 shows the EP inhibition of bacteria by nanoceria, evaluated by fluorescence of EtBr that resulted because of accumulation of EtBr in the cell. Treatment without iron-doped nanoceria was taken as a control.

4 Conclusion

The photosynthesised iron-doped nanoceria using extract of *F. vulgare* (fennel) seeds as capping and reducing agent presented fast, cost effective and environmental benign method. The dopant brought the activation of nanoceria to visible light from UV light. The TC-coated nanoceria annihilated the microbes found in real hospital effluent. The increase antimicrobial activity of nanoceria was proposed to occur as a result of oxidative stress caused by ROS, generated upon illumination with visible light. Furthermore, the coated nanoceria were found biocompatible (data not shown) and also showed significant efflux inhibitory activity. The current study was conducted on lab-scale and can be applied in field for the treatment of hospital as well as other effluent with microbial

contamination. Moreover, because of the enhanced antimicrobial activity, these nanoparticles can also be applied to viruses and fungi. Furthermore, these nanoparticles have strong potential for use as nano-filters and/or nano-adsorbents for the treatment of wastewater generated from both industries and hospital containing microorganisms.

5 Acknowledgments

6 References

[1] Wyasuh, G., Okerele, N.: 'The influence of hospital waste water samples grown within Ahmadu Bello University Teaching Hospital', *Adv. Appl. Sci. Res.*, 2012, **3**, (3), pp. 1686–1690

[2] Boillot, C., Bazin, A., Tissot-Guerraz, F., *et al.*: 'Daily physicochemical, microbiological and ecotoxicological fluctuations of a hospital effluent according to technical and care activities', *Sci. Total Environ.*, 2008, **403**, (1), pp. 113–129

[3] Verlicchi, P., Al Aukidy, M., Zambello, E.: 'What have we learned from worldwide experiences on the management and treatment of hospital effluent? — an overview and a discussion on perspectives', *Sci. Total Environ.*, 2015, **514**, pp. 467–491

[4] Laffite, A., Kilunga, P.I., Kayembe, J.M., *et al.*: 'Hospital effluents are one of several sources of metal, antibiotic resistance genes, and bacterial markers disseminated in Sub-Saharan urban rivers', *Front. Microbiol.*, 2016, **7**, p. 1128

[5] Almagor, J., Temkin, E., Benenson, I., *et al.*: 'The impact of antibiotic use on transmission of resistant bacteria in hospitals: insights from an agent-based model', *PloS One*, 2018, **13**, (5), pp. e0197111–e0197111

[6] Fischer, M.M., Bild, M.: 'Hospital use of antibiotics as the main driver of infections with antibiotic-resistant bacteria – a reanalysis of recent data from the European Union', bioRxiv, 2019, p. 553537

[7] Asfaw, T., Negash, L., Kahsay, A., *et al.*: 'Antibiotic resistant bacteria from treated and untreated hospital wastewater at Ayder Referral Hospital, Mekelle, North Ethiopia', *Adv. Microbiol.*, 2017, **7**, (12), p. 871

[8] Weinstein, R.A., Hota, B.: 'Contamination, disinfection, and cross-colonization: are hospital surfaces reservoirs for nosocomial infection?', *Clin. Infect. Dis.*, 2004, **39**, (8), pp. 1182–1189

[9] Manonmani, P., Raj, S.P., Ramar, M., *et al.*: 'Load of infectious microorganisms in hospital effluent treatment plant in Madurai', *South Indian J. Biol. Sci.*, 2015, **1**, (1), pp. 30–33

[10] Hocquet, D., Muller, A., Bertrand, X.: 'What happens in hospitals does not stay in hospitals: antibiotic-resistant bacteria in hospital wastewater systems', *J. Hosp. Infect.*, 2016, **93**, (4), pp. 395–402

[11] Adegoke, A.A., Amoah, I.D., Stenström, T.A., *et al.*: 'Epidemiological evidence and health risks associated with agricultural reuse of partially treated and untreated wastewater: a review', *Front. Public Health*, 2018, **6**, p. 337

[12] Ahsan, N.: 'Study of widely used treatment technologies for hospital wastewater and their comparative analysis', *Int. J. Adv. Eng. Technol.*, 2012, **5**, (1), p. 227

[13] Chitnis, V., Chitnis, S., Vaidya, K., *et al.*: 'Bacterial population changes in hospital effluent treatment plant in central India', *Water Res.*, 2004, **38**, (2), pp. 441–447

[14] Rizzo, L., Manaia, C., Merlin, C., *et al.*: 'Urban wastewater treatment plants as hotspots for antibiotic resistant Bacteria and genes spread into the environment: a review', *Sci. Total Environ.*, 2013, **447**, pp. 345–360

[15] Li, R., Jay, J.A., Stenstrom, M.K.: 'Fate of antibiotic resistance genes and antibiotic-resistant bacteria in water resource recovery facilities', *Water Environ. Res.*, 2019, **91**, (1), pp. 5–20

[16] Sharma, V.K., Johnson, N., Cizmas, L., *et al.*: 'A review of the influence of treatment strategies on antibiotic resistant bacteria and antibiotic resistance genes', *Chemosphere*, 2016, **150**, pp. 702–714

[17] Li, Y., Zhu, G., Ng, W.J., *et al.*: 'A review on removing pharmaceutical contaminants from wastewater by constructed wetlands: design, performance and mechanism', *Sci. Total Environ.*, 2014, **468–469**, pp. 908–932

[18] Masadeh, M.M., Karasneh, G.A., Al-Akhras, M.A., *et al.*: 'Cerium oxide and iron oxide nanoparticles abolish the antibacterial activity of ciprofloxacin against gram positive and gram negative biofilm bacteria', *Cytotechnology*, 2015, **67**, (3), pp. 427–435

[19] Caputo, F., Mameli, M., Sienkiewicz, A., *et al.*: 'A novel synthetic approach of cerium oxide nanoparticles with improved biomedical activity', *Sci. Rep.*, 2017, **7**, (1), p. 4636

[20] Farias, I.A.P., Santos, C.C.L.d., Sampaio, F.C., *et al.*: 'Antimicrobial activity of cerium oxide nanoparticles on opportunistic microorganisms: a systematic review', *BioMed Res. Int.*, 2018, **2018**, p. 14

[21] Arumugam, A., Karthikeyan, C., Hameed, A.S.H., *et al.*: 'Synthesis of cerium oxide nanoparticles using *Gloriosa superba* L. leaf extract and their structural, optical and antibacterial properties', *Mater. Sci. Eng., C*, 2015, **49**, pp. 408–415

[22] Das, S., Dowding, J.M., Klump, K.E., *et al.*: 'Cerium oxide nanoparticles: applications and prospects in nanomedicine', *Nanomedicine*, 2013, **8**, (9), pp. 1483–1508

[23] Baruah, S., Mahmood, M.A., Myint, M.T.Z., *et al.*: 'Enhanced visible light photocatalysis through fast crystallization of zinc oxide nanorods', *Beilstein J. Nanotechnol.*, 2010, **1**, p. 14

[24] Sohail, M.F., Javed, I., Hussain, S.Z., *et al.*: 'Folate grafted thiolated chitosan enveloped nanoliposomes with enhanced oral bioavailability and anticancer activity of docetaxel', *J. Mater. Chem. B*, 2016, **4**, (37), pp. 6240–6248

[25] Elumalai, K., Velmurugan, S.: 'Green synthesis, characterization and antimicrobial activities of zinc oxide nanoparticles from the leaf extract of Azadirachta indica (L.)', *Appl. Surf. Sci.*, 2015, **345**, pp. 329–336

[26] Nadhman, A., Nazir, S., Khan, M.I., *et al.*: 'Visible-light-responsive zncuo nanoparticles: benign photodynamic killers of infectious protozoans', *Int. J. Nanomed.*, 2015, **10**, pp. 6891–6903

[27] Channei, D., Inceesungvorn, B., Wetchakun, N., *et al.*: 'Photocatalytic degradation of methyl orange by CeO_2 and Fe–doped CeO_2 films under visible light irradiation', *Sci. Rep.*, 2014, **4**, p. 5757

[28] Nadhman, A., Nazir, S., Khan, M.I., *et al.*: 'Pegylated silver doped zinc oxide nanoparticles as novel photosensitizers for photodynamic therapy against *Leishmania*', *Free Radicals Biol. Med.*, 2014, **77**, pp. 230–238

[29] Christena, L.R., Mangalagowri, V., Pradheeba, P., *et al.*: 'Copper nanoparticles as an efflux pump inhibitor to tackle drug resistant bacteria', *RSC Adv.*, 2015, **5**, (17), pp. 12899–12909

[30] Iqbal, G., Faisal, S., Khan, S., *et al.*: 'Photo-inactivation and efflux pump inhibition of methicillin resistant Staphylococcus aureus using thiolated cobalt doped ZnO nanoparticles', *J. Photochem. Photobiol., B*, 2019, **192**, pp. 141–146

[31] Choudhary, M.K., Kataria, J., Sharma, S.: 'A biomimetic synthesis of stable gold nanoparticles derived from aqueous extract of Foeniculum vulgare seeds and evaluation of their catalytic activity', *Appl. Nanosci.*, 2017, **7**, (7), pp. 439–447

[32] Price, M., Reiners, J.J., Santiago, A.M., *et al.*: 'Monitoring singlet oxygen and hydroxyl radical formation with fluorescent probes during photodynamic therapy', *Photochem. Photobiol.*, 2009, **85**, (5), pp. 1177–1181

[33] Li, Y., Zhang, W., Niu, J., *et al.*: 'Mechanism of photogenerated reactive oxygen species and correlation with the antibacterial properties of engineered metal-oxide nanoparticles', *ACS Nano*, 2012, **6**, (6), pp. 5164–5173

[34] Maqbool, Q., Nazar, M., Naz, S., *et al.*: 'Antimicrobial potential of green synthesized CeO_2 nanoparticles from olea Europaea leaf extract', *Int. J. Nanomed.*, 2016, **11**, p. 5015

[35] Amaral, L., Martins, A., Spengler, G., *et al.*: 'Efflux pumps of gram-negative bacteria: what they do, how they do it, with what and how to deal with them', *Front. Pharmacol.*, 2014, **4**, p. 168